

Comparative *In Vitro* Anticancer Study of Cisplatin Drug with Green Synthesized ZnO Nanoparticles on Cervical Squamous Carcinoma (SiHa) Cell Lines

Nutan Rani, Kavita Rawat, Mona Saini, Sapna Yadav, Saima Syeda, Kalawati Saini,* and Anju Shrivastava*



Cite This: *ACS Omega* 2023, 8, 14509–14519



Read Online

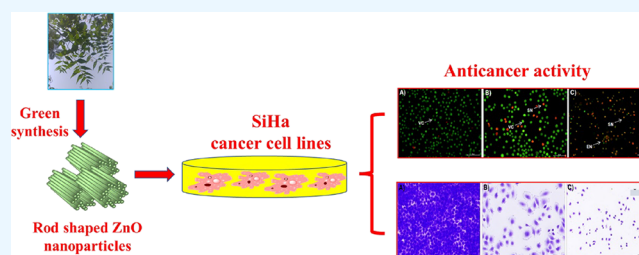
ACCESS |

Metrics & More

Article Recommendations

Supporting Information

ABSTRACT: In this article, we aimed to develop a unique treatment approach to cure cervical cancer without harming healthy normal cells and overcome the limitations of currently available therapies/treatments. Recently, chemotherapeutics based on metal oxides have gained attention as a promising approach for treating cancer. Herein, ZnO nanoparticles were synthesized with the leaf extract of *Azadirachta indica*. These green synthesized ZnO nanoparticles were used for a cytotoxic study on the cervical squamous carcinoma cell line SiHa and murine macrophage cell line RAW 264.7. Moreover, a hemolytic assay was performed to check the biocompatibility of ZnO nanoparticles. The biosynthesized ZnO nanoparticles were labeled as L1, L2, L5, and L10 nanoparticles. Various assays like crystal violet, MTT assay, and AO/PI dual staining method were performed to assess the anticancer potential of ZnO. The concentration of ZnO nanoparticles was taken in the range of 100–250 $\mu\text{g}/\text{mL}$ in the *in vitro* anticancer study on SiHa cancer cell lines. The findings of the MTT assay revealed that biosynthesized ZnO nanoparticles exhibited significant cytotoxicity against SiHa cancer cell lines dose-dependently at two incubation times (24 and 48 h). Also, a decrease in cell viability was observed with an increased concentration of ZnO. The IC_{50} values obtained were 141 $\mu\text{g}/\text{mL}$ for L1, 132 $\mu\text{g}/\text{mL}$ for L2, 127 $\mu\text{g}/\text{mL}$ for L5, and 115 $\mu\text{g}/\text{mL}$ for L10 nanoparticles. In addition, cisplatin drug (10 $\mu\text{g}/\text{mL}$) was also used to compare the anticancer activity with the biosynthesized L1, L2, L5, and L10 nanoparticles. The results of the crystal violet assay and AO/PI dual staining method revealed that morphological changes like cell shrinkage, poor cell adhesion, and induction of apoptosis occurred in the SiHa cancer cell lines. Furthermore, the stability of the ZnO nanoparticles at physiological pH has been assessed by recording the UV–visible spectrum at various pH values. Hence, the overall findings suggested that biosynthesized ZnO nanoparticles can be utilized for cervical squamous cancer treatment in addition to the current treatment strategies/techniques.



1. INTRODUCTION

A root cause of mortality worldwide today is cancer. Cancer, which is the world's biggest health issue, has an equal impact on both developing and undeveloped countries. Globally, the second most frequent cancer among females is cervical cancer. Every year, about 400,000 new cases of this cancer are detected, and nearly half of them will be fatal.¹ The majority (80–90%) of cervical malignancies are squamous cell carcinomas, whereas adenocarcinomas account for the remaining 20% of cervical cancer occurrences.² High-risk variants of human papillomaviruses (HPV) are the leading causes of the overwhelming majority of cases of cervical cancer. There are currently a variety of therapies available for cancer treatment, including hormonal therapy, immunotherapy, radiation therapy, and chemotherapy. The choice of therapy selection is made depending on the patient's physical condition, location, status, and stage of cancer. But many of the treatments/therapies discussed above are associated with serious adverse effects. As a result, there is an urgent need to

develop novel therapeutic strategies with enhanced theranostic potential and minimal side effects.

A new field of research in cancer therapeutic strategies has been made possible by major developments in nanotechnology.^{3,4} Various metal oxide nanoparticles have been studied and reported in the literature for their anticancer potential.^{5–8} However, zinc oxide nanoparticles (due to their unique properties) have been considered very significant among the numerous metal oxide nanoparticles.⁹ ZnO nanoparticles are potent multifunctional wide band gap n-type semiconductors. As a result of a suitable band gap, ZnO nanoparticles can easily

Received: January 3, 2023

Accepted: March 28, 2023

Published: April 12, 2023



generate reactive oxygen species (ROS). The tendency of ZnO nanoparticles to generate ROS makes them suitable for anticancer studies. Moreover, the higher selective anticancer activity of ZnO nanoparticles toward tumor cells at physiological pH is another important reason that makes them a preferable candidate for anticancer studies. These nanoparticles show a cytotoxic behavior toward cancer cells, and no effects have been observed against normal cell lines. The literature survey depicted that ZnO nanoparticles exhibit selective *in vitro* cytotoxic potential against various cancer cell lines.^{29–31} Hence, the unique properties of ZnO nanoparticles such as biocompatibility, ease of fabrication, nontoxicity, excellent selectivity, and improved cytotoxicity are responsible for making ZnO nanoparticles a better candidate for anticancer studies.³²

A vast number of applications are reported for zinc oxide nanoparticles in various fields.^{10–13} As reported by Dhawan and Chadha, zinc deficiency promotes the growth of malignancy, whereas zinc supplementation inhibits and prevents cancers of the colon, pancreas, and esophagus.¹⁴ The synthesis of zinc oxide nanoparticles from various medicinal plants and their effectiveness against various cancer cell lines have both been investigated and reported in several literature reports.^{15–19} The cytotoxic effect of *Candelabra cactus* flower extract-mediated zinc oxide nanoparticles against MCF-7 cells has been studied.²⁰ Herein, zinc oxide nanoparticles showed excellent apoptosis. In addition, cell viability declined with an increment in the concentration of zinc oxide nanoparticles. Naser et al. have reported the cytotoxic effect of *Phoenix dactylifera* root hair extract-mediated zinc oxide nanoparticles.²¹ In this article, the cytotoxicity of ZnO nanoparticles was found to be more than that of the anticancer drug doxorubicin (DOX) against breast cancer cells (TNBC). ZnO nanoparticles obtained nearly 45% higher cytotoxicity than doxorubicin (DOX). Furthermore, the cytotoxic effect of this ZnO was 82.26% on human lung cancer (A549) cells. Wu and Zhang studied the anticancer effect of chitosan-assembled zinc oxide nanoparticles against human cervical carcinoma (HeLa) cancer cell lines.²² The cytotoxicity was determined based on the reactive oxygen species (ROS).

In this study, our goal is to investigate an alternative and better therapeutic agent that could enhance the efficiency of treatment for cervical cancer cells. In this article, we have presented the *in vitro* cytotoxic study of biosynthesized ZnO using the leaf extract of *Azadirachta indica*. The cervical squamous carcinoma (SiHa) cancer cell line was utilized to observe the cytotoxic effect. In addition, the cisplatin drug was also used for comparative *in vitro* anticancer studies with green synthesized ZnO nanoparticles.

2. EXPERIMENTAL SECTION

2.1. Leaf Extract Mediated Biosynthesis of ZnO NPs.

Rani et al. have already reported the experimental procedure for the biosynthesis of zinc oxide nanoparticles using an aqueous leaf extract of *Azadirachta indica*.^{23–25} The as-synthesized zinc oxide nanoparticles were labeled as L1, L2, L5, and L10 corresponding to the volume of leaf extract taken as 1.0, 2.0, 5.0, and 10.0 mL, respectively.

2.2. Cytotoxic Study. **2.2.1. Materials Required.** DMSO and methyl alcohol were acquired from SRL, India. SiHa (cervical squamous cancer) cell lines and murine macrophage (RAW 264.7) cell lines were purchased from the National Cell Repository of Animal Cells NCCS (Pune), India. MTT and

DMEM were obtained from Sigma Aldrich, USA. FBS was procured from Invitrogen. PI, RNase, AO, and CV were acquired from Bangalore Genei.

2.2.2. SiHa Cancer Cell Culture. SiHa cancer cells were cultivated in DMEM containing 10% (v/v) heat-inactivated FBS. After that, all cultures were incubated at 37 °C in the presence of 5% CO₂ and a humid environment. Following that, the SiHa cells were passaged once every 2 to 3 days, and a logarithmic growth phase of SiHa cancer cell lines was taken to conduct various assays. The various experiments/assays such as the MTT assay, CV assay, and AO/PI assay were performed with different concentrations of ZnO (L1, L2, L5, and L10) and cisplatin drug at incubation times of 24 and 48 h, respectively.

2.2.3. Assessment of Viability Using the MTT Assay. The viability of SiHa cells was determined with L1, L2, L5, and L10 nanoparticles and cisplatin drug by the MTT assay. Yellow-colored soluble MTT is converted into purple-colored insoluble formazan through the breaking of the tetrazolium ring by enzymes (mitochondrial dehydrogenase) present in the living cells. Hence, this assay reflects the proportion of viable cells. This activity is not expressed by dead cells. In brief, 96-well plates were inoculated with 5×10^4 cells per well, incubated overnight, and then allowed to acclimatize in DMEM (5% CO₂) at 37 °C. After that, these SiHa cells were exposed to various concentrations (100, 150, 200, and 250 µg/mL) of L1, L2, L5, and L10 nanoparticles in the incubator (CO₂) for incubation times of 24 and 48 h at 37 °C. After that, the culture media were discarded for 4 h prior to the completion of the experiment and substituted with fresh medium (180 µL) and 20 µL (5 mg/mL in PBS) of MTT solution. After that, the incubation of the 96-well plates was done at 37 °C for the remaining 4 h in the dark with CO₂ and a humidified atmosphere. Finally, after the removal of media, the as-formed formazan crystals were dissolved by adding 100 µL per well of DMSO. The optical density (OD) value was recorded at 570 nm with a microplate spectrophotometer (BIO-TEK, USA). The IC₅₀ value was obtained by the linear regression of the dose- and time-dependent curve. Furthermore, the % cell viability was determined using the equation below:

$$\% \text{Cell viability} = (\text{OD value of treated sample} / \text{OD value of control sample}) \times 100$$

2.2.4. Assessment of Morphology Using the CV Assay.

The crystal violet assay was performed for determining the shapes and sizes of SiHa cell lines. The IC₅₀ dose of green synthesized ZnO nanoparticles was determined with the MTT assay and utilized to treat the abovementioned cell lines throughout the experiments. In brief, SiHa cell lines were plated in a six-well plate and kept overnight for sticking without disturbance. After that, the adhered cells were exposed to the corresponding IC₅₀ dose of green synthesized L1, L2, L5, and L10 nanoparticles for an incubation time of 48 h. After that, the medium was discarded, and cell lines were rinsed by PBS three times. Following that, SiHa cell lines were fixed for 1 min duration in the presence of 100% methanol. After that, the SiHa cell lines were stained with CV for 50–55 s duration. Later on, the plate was rinsed with normal water three times and left for drying in the air. Finally, stained SiHa cell lines were observed and imaged at 200× magnification through a Nikon microscope. The difference in shapes and sizes of SiHa

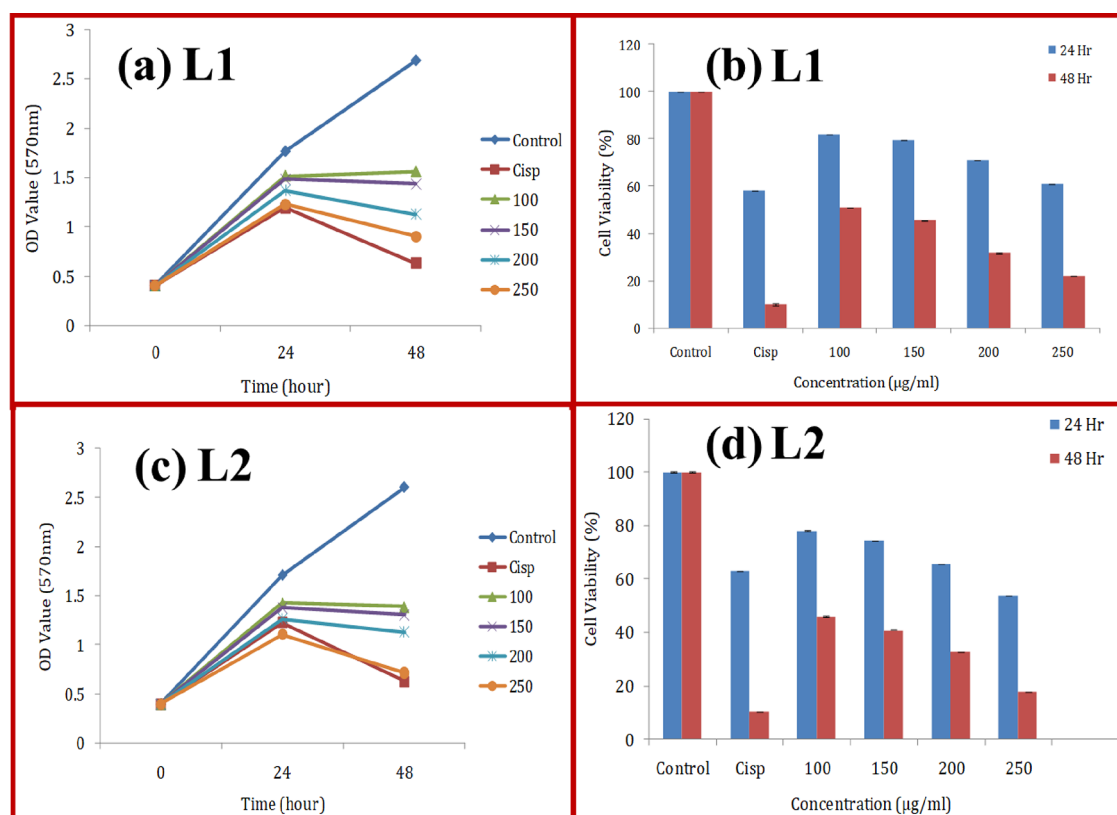


Figure 1. (a, c) Optical density (OD) values of SiHa cells treated with different concentrations of L1 and L2 nanoparticles, respectively, at time intervals of 24 h and 48 h. Data are depicted in triplicate by performing three separate experiments. (b, d) The corresponding cell viability graphs of SiHa cells treated with L1 and L2 nanoparticles, respectively. Data are shown as mean \pm SD.

cell lines was determined and compared with the control cells that were not treated with green synthesized nanoparticles.

2.2.5. Assessment of Apoptosis Using the AO/PI Staining Method. To determine how ZnO nanoparticles impacted the viability of SiHa cells to undergo apoptosis, a twofold AO/PI staining analysis approach was performed. In brief, SiHa cell lines were plated in six-well plates, and incubation was done overnight for adhering. Following that, the SiHa cell lines were incubated with L1, L2, L5, and L10 nanoparticles at the relevant IC_{50} dose for 48 h. The SiHa cell lines were washed after incubation by PBS two times. Afterward, centrifugation was done at 1500 rpm for 3 min. After that, the cell lines were suspended again in PBS (cold) and centrifuged one more time to get clean and fresh cell pellets. After that, these fresh and cleaned pellets were mixed with an equal volume of AO and PI fluorescent dye staining solution made in PBS. The freshly stained cell suspension was dropped onto a clean glass slide and covered with a coverslip for the uniform distribution of cells. The stained SiHa cell lines with AO and PI fluorescent dye were imaged within 30 min before the fluorescence faded off through the UV-fluorescence microscope.

2.2.6. Assessment of Cytotoxic Studies Using Statistical Analysis. The analysis of all cytotoxic outcomes of SiHa cell lines was performed by one-way ANOVA that was followed by Dunnett's multiple comparison tests. For further analysis, the GraphPad Prism 6 version software was utilized. A statistically significant value was determined to be $p < 0.05$.

2.2.7. Assessment of the Biocompatibility of Synthesized ZnO (L1, L2, L5, L10) Using the Hemolytic Assay. To assess the biocompatibility of ZnO nanoparticles (L1, L2, L5, and L10) with blood cells, a hemolytic assay was performed.²

Blood samples were collected from healthy individuals in EDTA-coated vials. The blood was then transferred to 15 mL Falcon tubes and diluted with sterile PBS (1:2). The Falcon tubes were then centrifuged at 3000 rpm for 15 min, and the isolated erythrocytes were washed with PBS. Finally, the erythrocytes were suspended in a 10 mL PBS solution. After that, 200 μ L of the cell suspension was taken and treated with different concentrations of ZnO nanoparticles (100–250 μ g/mL) for 1 h at 37 $^{\circ}$ C and kept for incubation. The cell suspension treated with PBS and with 0.2% Triton X-100 was used as a negative and positive control, respectively. After incubation, the suspension was centrifuged at 3000 rpm for 5 min, and the absorbance of each cell supernatant was taken at 577 nm using the microplate spectrophotometer (BIO-TEK, USA). Percent hemolysis was calculated using the equation below:

$$\text{Percent hemolysis} = (A_T - A_{NC}) / (A_{PC} - A_{NC}) \times 100$$

In the above equation, the terms used were as follows: A_T , absorbance of the test sample; A_{NC} , absorbance of the negative control; and A_{PC} , absorbance of positive control.

3. RESULTS AND DISCUSSION

3.1. Viability of SiHa Cell Lines on Treatment with ZnO (L1, L2, L5, and L10) and Cisplatin Drug. The viability of SiHa cell lines was determined to investigate the impact of green synthesized (L1, L2, L5, and L10) nanoparticles and cisplatin drug using the MTT assay. The microplate reader was used to record the OD (optical density) value at 570 nm. In this study, viable numbers of cell lines were

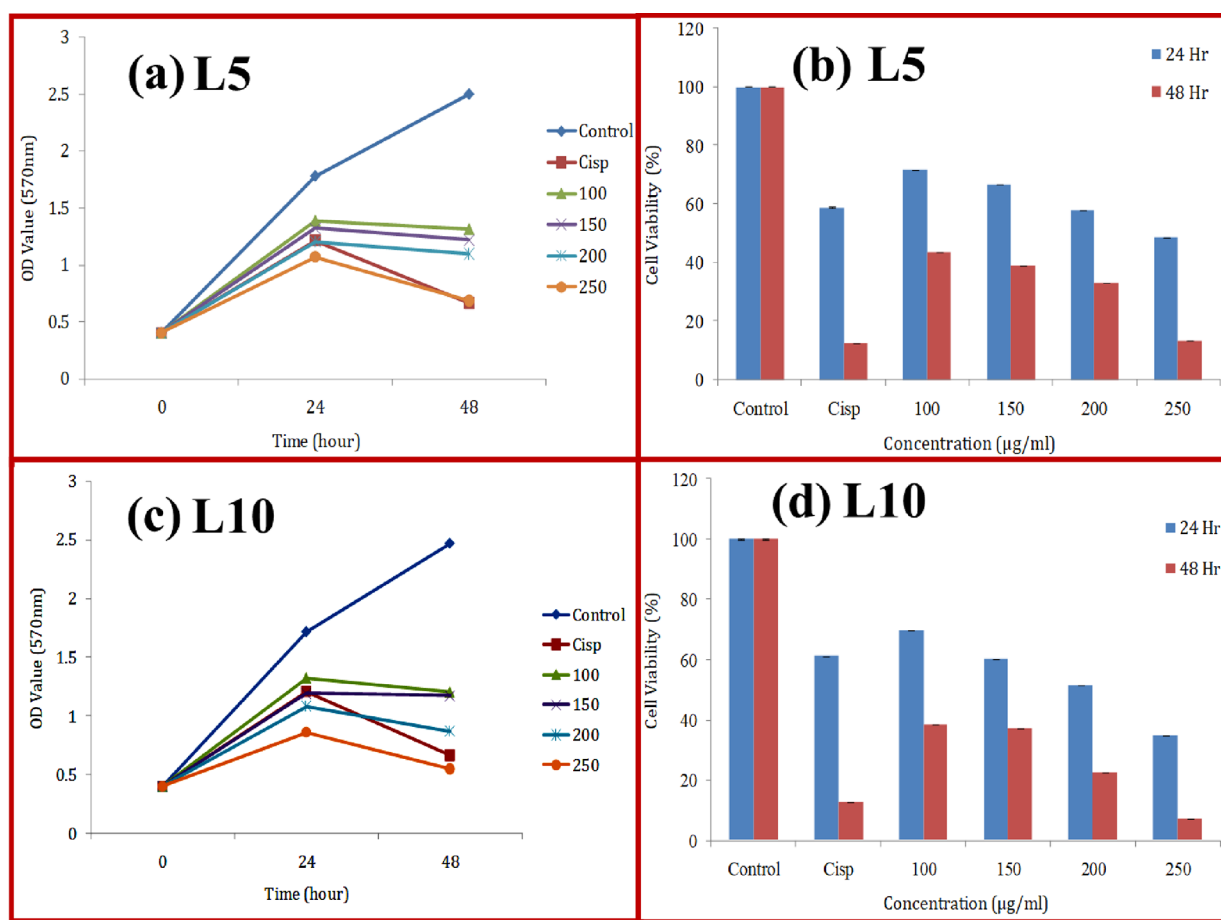


Figure 2. (a, c) Optical density (OD) values of SiHa cells treated with different concentrations of L5 and L10 nanoparticles, respectively, at time intervals of 24 h and 48 h. Data are depicted in triplicate by performing three separate experiments. (b, d) The corresponding cell viability graphs of SiHa cells treated with L5 and L10, respectively. Data are shown as mean \pm SD.

determined at 24 and 48 h, respectively. A higher percentage of living cells was indicated by a high OD value. The OD values of the SiHa cell lines are shown in Figure 1a,c. Herein, concentrations of L1 and L2 nanoparticles varying from 100 to 250 $\mu\text{g/mL}$ and 10 $\mu\text{g/mL}$ of cisplatin drug were used at up to 48 h time intervals, respectively. The cell viability of SiHa cell lines with L1 and L2 nanoparticles is given in Figures 1b,d, respectively. It is clear from these cell viability data that the cytotoxic effect of the cisplatin drug is found to be more than the L1 and L2 nanoparticles.

Similarly, the OD values of the SiHa cell lines are shown in Figures 2a,b, respectively. In this study, the SiHa cell lines were treated with green synthesized L5 and L10 nanoparticles. Concentrations of these nanoparticles varying from 100 to 250 $\mu\text{g/mL}$ and 10 $\mu\text{g/mL}$ of cisplatin drug were utilized at a 48 h time period. The cell viability is shown in Figures 2b,d, respectively, with green synthesized L5 and L10 nanoparticles.

It is noticeable that the viability of SiHa cell lines diminishes as the concentration of ZnO (L1, L2, L5, and L10) increases. Herein, the viability of these cell lines depends on dose and time, respectively, with all synthesized nanoparticles. Additionally, the 48 h incubation time results in a considerable reduction in cell viability at the numerous utilized concentrations (100, 150, 200, and 250 $\mu\text{g/mL}$) of green synthesized nanoparticles. As compared to cisplatin, the concentration used for synthesized ZnO nanoparticles is too much because the criterion for the selection of dose amount corresponds to the

IC_{50} value. Furthermore, we selected the IC_{50} dose for ZnO nanoparticle (L1, L2, L5, and L10) treatment after performing the dose kinetics. IC_{50} is a quantitative measure that shows how much of a particular inhibitory drug is needed to inhibit a given biological process by 50% *in vitro* in pharmacological research. In the case of cisplatin, a high dose is avoided because it leads to several side effects such as systemic toxicity, renal toxicity, vomiting, gastrointestinal toxicity, and many more.³³ Our ZnO nanoparticles were synthesized using the aqueous leaf extract of *Azadirachta indica*; so, comparatively, they are less toxic than cisplatin. Moreover, several studies reported that ZnO nanoparticles synthesized using plant materials/extracts are safe, biocompatible, and nontoxic.^{34,35} The IC_{50} values of all the synthesized ZnO are given in Table 1. From the IC_{50} values, we can conclude that as the amount (volume) of leaf extract increases for the green synthesized nanoparticles, % cell viability decreases accordingly. Furthermore, the cytotoxic

Table 1. Values of IC_{50} with Various Green Synthesized Nanoparticles Obtained from the MTT Assay

s. no.	ZnO nanoparticles	IC_{50} ($\mu\text{g/mL}$)
1	L1	141
2	L2	132
3	L5	127
4	L10	115

Table 2. Comparative Study with Reported Nanomaterials for Cervical Squamous Carcinoma (SiHa) Cell Lines in the Literature

s. no.	nanomaterials used	synthesis method	cancer cell lines used	size and morphology	incubation time/IC ₅₀	references
1	1,10-phenanthroline coupled ZnO nanoparticles	sol-gel and precipitation method	SiHa cervical	hexagonal tube-shaped and sphere-like particles	48 h	36
2	zinc oxide nanoparticles	biosynthesis method (<i>Lantana aculeata</i> L.)	SiHa cervical	spherical	24 h/48.16 $\mu\text{g/mL}$	37
3	chitosan nanoparticles	biosynthesis method	SiHa cervical	spherical	24 h/102.17 $\mu\text{g/mL}$	38
4	silver nanoparticles	biosynthesis method (<i>Withania coagulans</i>)	SiHa cervical	spherical	48 h/13.74 $\mu\text{g/mL}$	39
5	vanadium nanoparticles	biosynthesis method (<i>Calendula officinalis</i>)	SiHa cervical	spherical	72 h/259 $\mu\text{g/mL}$	40
6	tin oxide nanoparticles	biosynthesis method (<i>Limonia acidissima</i>)	SiHa cervical	quasi-spherical	24 h/35 \pm 0.03 $\mu\text{g/mL}$	41
7	silver nanoparticles	biosynthesis method (<i>Delonix regia</i>)	SiHa cervical	nonuniform	48 h/15.96 $\mu\text{g/mL}$,	42
8	platinum nanoparticles	biosynthesis method (tea polyphenol)	SiHa cervical	flower-shaped	24 h/18.34 $\mu\text{g/mL}$	43
9	zinc oxide nanoparticles	biosynthesis method (<i>Azadirachta indica</i>)	SiHa cervical	rod- and sheet-shaped		present work

effect of L10 nanoparticles has been found to be more pronounced than the used standard drug cisplatin.

Similarly, other research groups have published comparable experiments on various cancer cell lines by utilizing biosynthesized ZnO nanoparticles.^{26–28} Table 2 depicts the comparative study with the reported nanomaterials for cervical squamous carcinoma (SiHa) cell lines in the literature.

3.2. Morphological Changes in SiHa Cells upon Treatment with Green Synthesized L1, L2, L5, and L10 Nanoparticles and Cisplatin Drug. The impact of biosynthesized ZnO and cisplatin drug on the morphology of SiHa cells was evaluated using a crystal violet (CV) assay. These cell lines stained with CV dye were imaged through a Nikon microscope at 200 \times magnification. Obtained images of the abovementioned cell lines are shown in Figure 3a,b after treating with green synthesized L1 and L2 nanoparticles, respectively. Figure 4a,b depicts the images of CV-stained SiHa cell lines treated with L5 and L10. The SiHa cell lines have been exposed to the ZnO at their corresponding IC₅₀ dose (as mentioned in Table 1), respectively, for 48 h.

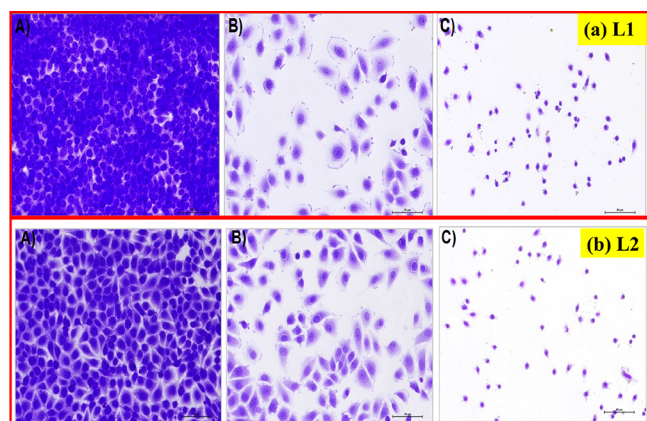


Figure 3. (a, b) Morphology of SiHa cell lines after treatment with L1 and L2 nanoparticles, respectively. (A) Control group (without treatment), (B) standard drug cisplatin-treated SiHa cell lines, and (C) SiHa cell lines treated with green synthesized L1 and L2 nanoparticles (at IC₅₀) at 200 \times magnification.

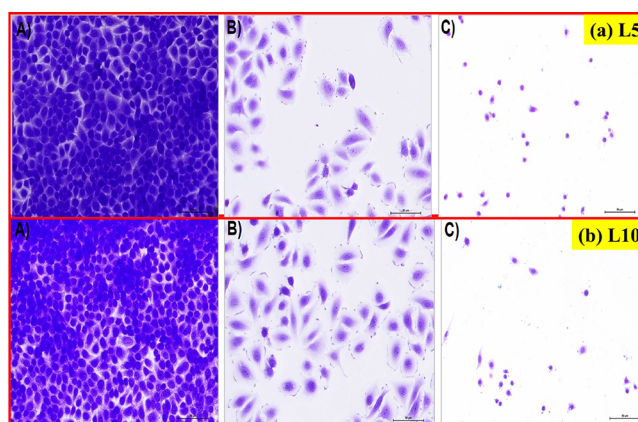


Figure 4. (a, b) Morphology of SiHa cells after treatment with L5 and L10 nanoparticles, respectively. (A) Control group (without treatment), (B) standard drug cisplatin-treated SiHa cells, (C) SiHa cell lines treated with green synthesized L5 and L10 nanoparticles (at IC₅₀) at 200 \times magnification.

The obtained micrographs revealed the morphological changes such as the shrinking of cells followed by the rounded shape of cells, decline in cell number, and weak cell adherence that resulted from the treatment with L1, L2, L5, and L10 nanoparticles. Similar morphological changes happened in the SiHa cell lines that were treated with the standard drug cisplatin. In addition, the number of SiHa cell lines remained the same after treatment with the cisplatin drug. But the number of SiHa cell lines has decreased on exposure to green synthesized L1, L2, L5, and L10 nanoparticles. Moreover, it is clear from the results that the toxic effect of L10 nanoparticles on the morphology of SiHa cell lines has been obtained the highest among all the synthesized nanoparticles.

3.3. Morphological Changes in Murine Macrophage Cell Line RAW 264.7 upon Treatment with Green Synthesized L1, L2, L5, and L10 Nanoparticles and Cisplatin Drug. To test the effect of green synthesized ZnO nanoparticles on normal cell lines, we utilized the murine macrophage cell line RAW 264.7. An alteration in the morphology is the key characteristic of macrophages that changes in accordance with their polarization. Inactivated macrophages show round, more or less spherical morphology,

whereas activation or inflammatory conditions induce them to become more flattened with an expanded cytoplasm. Figure 5

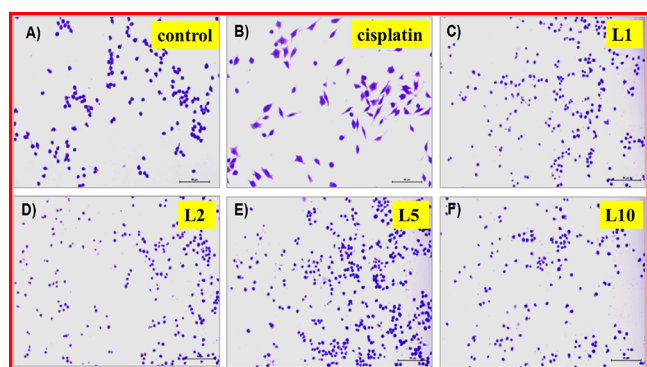


Figure 5. Morphology of the murine macrophage cell line (RAW 264.7) after treatment with ZnO nanoparticles. (A) Control group (without treatment), (B) standard drug cisplatin-treated cells, (C) cells treated with IC₅₀ dose (141 $\mu\text{g}/\text{mL}$) of L1, (D) cells treated with IC₅₀ dose (132 $\mu\text{g}/\text{mL}$) of L2, (E) cells treated with IC₅₀ dose (127 $\mu\text{g}/\text{mL}$) of L5, and (F) cells treated with IC₅₀ dose (115 $\mu\text{g}/\text{mL}$) of L10 at 200 \times magnification.

depicts the morphology of murine macrophage cell lines (RAW 264.7) after treatment with ZnO nanoparticles. We observed a round cell morphology in the control group as well as in the group treated with green synthesized ZnO nanoparticles (L1, L2, L5, and L10), whereas macrophages looked more flattened with more phagocytic extensions in the cisplatin-treated group, showing the activated state of macrophages. Furthermore, AO/PI staining also showed signs of cell death such as secondary necrosis (SN) and early necrosis (EN).

3.4. Apoptosis Induction in SiHa Cells upon Treatment with L1, L2, L5, and L10 Nanoparticles and Cisplatin Drug. The induction of apoptosis can be ensured by examining carefully the particular changes that happened in the morphological description of the SiHa cell lines. These particular changes include chromatin condensation, shrinking of the cells, and nuclear or cytoplasmic fragmentations. Acridine orange (AO) and propidium iodide (PI) dual staining studies have been carried out for validating the induction of apoptosis in SiHa cell lines. The dead cell lines are revealed by PI staining, whereas nonmalignant cell lines or early apoptotic cells with fragmented DNA are displayed through AO staining. Fluorescent (AO/PI) images of SiHa cell lines are presented in Figure 6a,b, respectively. These cell lines interacted with IC₅₀ doses of 141 $\mu\text{g}/\text{mL}$ for L1 and 132 $\mu\text{g}/\text{mL}$ for L2 nanoparticles, respectively. Similarly, the fluorescent (AO/PI) images of SiHa cell lines are shown in Figure 7 a,b, respectively. Herein, the treatment of these cell lines was done with IC₅₀ doses of 127 $\mu\text{g}/\text{mL}$ for L5 and 115 $\mu\text{g}/\text{mL}$ for L10 nanoparticles.

Following that, SiHa cell lines were examined for determining various phases of cells like viable cells and early/late apoptotic phases through the fluorescent microscope. We found signs of cell death such as secondary necrosis (SN), chromatin condensations (CC), and early apoptosis (EA) in SiHa cell lines after treatment with L1, L2, L5, and L10 nanoparticles, respectively. The presence of green-colored unbroken nuclei in the SiHa cell lines indicates viable cells after 48 h incubation time. This indicates that no apoptosis

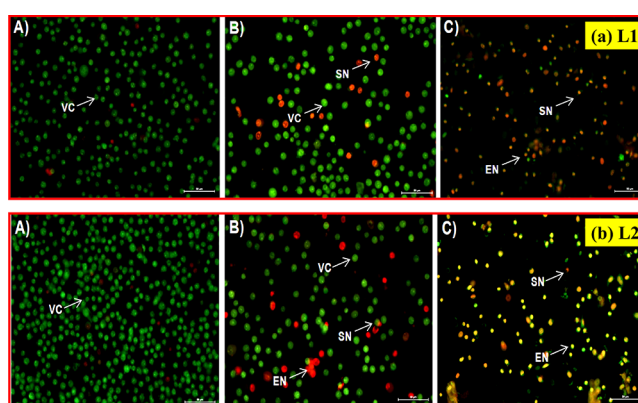


Figure 6. Shape and size determination of SiHa cell lines (AO/PI stained). (a) The treated SiHa cell lines with an IC₅₀ dose of L1 nanoparticles (141 $\mu\text{g}/\text{mL}$) for 48 h. (A) SiHa cell lines without treatment, (B) SiHa cell lines treated with cisplatin, and (C) SiHa cell lines treated with L1 nanoparticles. (b) The treated SiHa cell lines with an IC₅₀ dose of L2 nanoparticles (132 $\mu\text{g}/\text{mL}$) for 48 h incubation time. VC: viable cells; EA: early apoptosis; and SN: secondary necrosis.

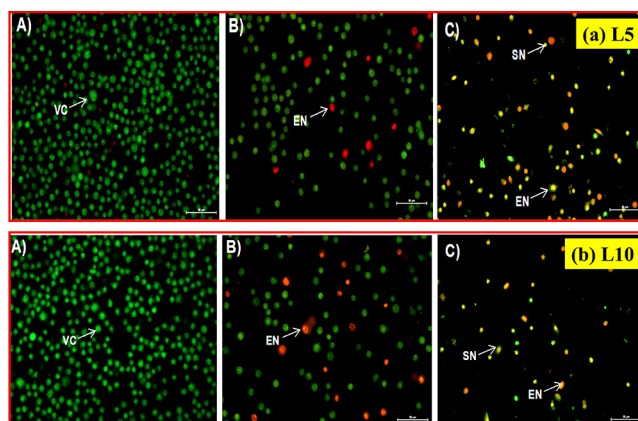


Figure 7. Shape and size determination of SiHa cell lines (AO/PI stained). (a) The treated SiHa cell lines with an IC₅₀ dose of L5 nanoparticles (127 $\mu\text{g}/\text{mL}$) for 48 h. (A) SiHa cell lines without treatment, (B) SiHa cell lines treated with cisplatin, and (C) SiHa cell lines treated with L5 nanoparticles. (b) The treated SiHa cell lines with an IC₅₀ dose of L10 nanoparticles (115 $\mu\text{g}/\text{mL}$) for 48 h. VC: viable cells; EA: early apoptosis; and SN: secondary necrosis.

took place in these cell lines. Furthermore, EA and SN stages were observed in all other cases at their corresponding IC₅₀ doses of green synthesized nanoparticles. The changes in shapes and sizes ensured the initiation of apoptosis in SiHa cell lines after exposure to L1, L2, L5, and L10 nanoparticles. Figure 8 depicts the AO/PI stained shape and size determination of murine macrophage (RAW 264.7) cell lines: (A) control group (without treatment), (B) standard drug cisplatin-treated cells, (C) cells treated with IC₅₀ dose (141 $\mu\text{g}/\text{mL}$) of L1, (D) cells treated with IC₅₀ dose (132 $\mu\text{g}/\text{mL}$) of L2, (E) cells treated with IC₅₀ dose (127 $\mu\text{g}/\text{mL}$) of L5, and (F) cells treated with IC₅₀ dose (115 $\mu\text{g}/\text{mL}$) of L10 ZnO nanoparticles.

The primary determining cause of apoptosis in many tumors is believed to be oxidative stress. Mostly, oxidative stress caused by ROS formation is considered to be a potent mechanism of cytotoxic activity exhibited by biogenic zinc

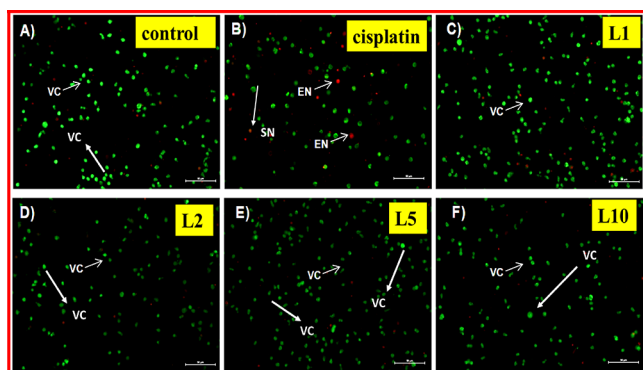


Figure 8. Shape and size determination of murine macrophage (RAW 264.7) cell lines (AO/PI stained). (A) Control group (without treatment), (B) standard drug cisplatin-treated cells, (C) cells treated with IC₅₀ dose (141 $\mu\text{g}/\text{mL}$) of L1, (D) cells treated with IC₅₀ dose (132 $\mu\text{g}/\text{mL}$) of L2, (E) cells treated with IC₅₀ dose (127 $\mu\text{g}/\text{mL}$) of L5, and (F) cells treated with IC₅₀ dose (115 $\mu\text{g}/\text{mL}$) of L10 for 48 h incubation time. VC: viable cells; EA: early apoptosis; and SN: secondary necrosis.

oxide nanoparticles on cancerous cells. Numerous typical metabolic processes are strongly influenced by oxidative stress.

The ROS generated by ZnO nanoparticles would interact with macromolecules like proteins, enzymes, and lipids and with DNA also. These interactions could result in variations, denaturation, and oxidations that would ultimately cause the degradation and dysfunction of different cellular organelles. Furthermore, DNA damage can inhibit healthy cells from performing their usual functions, which can lead to tumors or induction of apoptosis. Figure 9 depicts the schematic representation of mechanistic pathways for anticancer activity shown by ZnO nanoparticles.

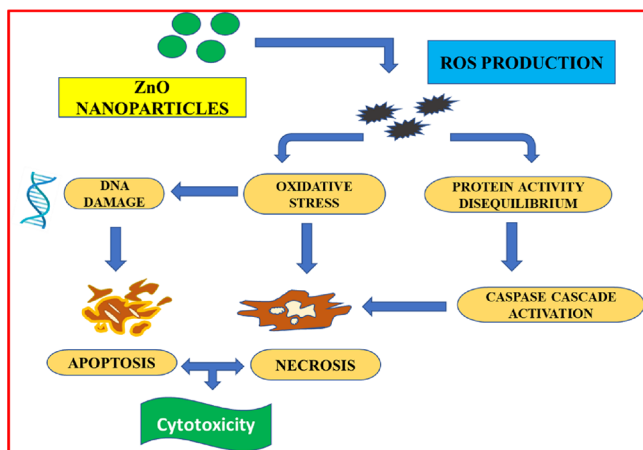


Figure 9. Schematic representation of mechanistic pathways for anticancer activity shown by ZnO nanoparticles.

3.5. Assessment of the Stability of Green Synthesized ZnO (L1, L2, L5, and L10) Nanoparticles at Different pH Values. The UV–visible spectra of ZnO nanoparticles (L1, L2, L5, and L10) were recorded to determine the stability at different pH values. Figure 10 a–c depicts the various UV–vis spectra recorded at pH 3, 5, and 7.4, respectively. At pH 3, there was no absorbance peak observed, whereas at pH 5 and 7.4, all the synthesized ZnO nanoparticles (L1, L2, L5, and

L10) exhibited absorbance maxima. The λ_{max} values are listed for all the synthesized ZnO nanoparticles in Table 3.

3.6. UV–Visible Spectroscopic Analysis. UV–visible spectra for the synthesized ZnO (L1, L2, L5, and L10) at pH = 7.4 in PBS are shown in Figure 10c. As the amount of the extract increased for the synthesis of ZnO nanoparticles, we observed that the band gap energy decreased. The band gap energy for the various synthesized ZnO nanoparticles was obtained as 2.86 eV for L1, 2.80 eV for L2, 2.34 eV for L5, and 2.28 eV for L10, respectively (as given in Figure 11 and Table 4). We have observed that the cytotoxic effect increased as the band gap decreased for the synthesized ZnO nanoparticles (L1, L2, L5, and L10) nanoparticles. Similarly, Arakha et al. have also reported that the cytotoxic effect of ZnO nanoparticles increased with the decreased band gap energy values.⁴⁴

3.7. Assessment of *In Vitro* Hemolytic Effect of Green Synthesized ZnO (L1, L2, L5, and L10) Nanoparticles on Erythrocytes. Hemolysis is an important screening test to ascertain the biocompatibility of compounds. A high degree of hemolysis by a compound means massive breakage of erythrocytes and thus represents low compatibility of that compound with blood. In the present study, we were interested to assess the blood compatibility of green synthesized ZnO nanoparticles (L1, L2, L5, and L10). We performed the hemolytic assay wherein erythrocytes were treated with different concentrations of L1, L2, L5, and L10. We used erythrocytes suspended in sterile PBS as negative control and in 0.2% Triton X-100 as positive control. The inset of Figure 12 a,b represents the photographs showing no significant hemolysis even at higher concentrations of L1 and L2, i.e., at 250 $\mu\text{g}/\text{mL}$, and was comparable to the negative control group. Hemolysis is determined by the presence of hemoglobin content reflected by the red color in the supernatant. In our study, with different concentrations of L1 and L2, hemoglobin content was found to be comparable to the negative control group in the supernatant. In contrast, the positive control group showed complete lysis of erythrocytes resulting in the release of hemoglobin in the supernatant. Bar graphs in Figure 12 a,b represent the corresponding percent hemolysis with different concentrations of L1 and L2, which was found to be less than 1% compared to the positive control group wherein we observed 100% hemolysis. Similarly, the inset of Figure 13 a,b represents the photographs showing no significant hemolysis even at higher concentrations of L5 and L10, i.e., at 250 $\mu\text{g}/\text{mL}$, and was comparable to the negative control group. Bar graphs of Figure 13 a,b represent the corresponding percent hemolysis with different concentrations of L5 and L10, which was found to be less than 1% compared to the positive control group wherein we observed 100% hemolysis. Our results revealed that green synthesized (L1, L2, L5, and L10) nanoparticles are nontoxic even at their higher concentrations.

4. CONCLUSIONS

In the current reported work, the *in vitro* cytotoxicity of green synthesized nanoparticles (L1, L2, L5, and L10) has been examined on SiHa cervical cancer cell lines via assays like CV, MTT, and acridine orange/propidium iodide assay. In addition, the standard anticancer drug cisplatin has also been used to compare the anticancer effect. Also, the cytotoxic effect has been evaluated on the murine macrophage cell line RAW 264.7 (normal cell lines). The IC₅₀ values for all the biosynthesized ZnO nanoparticles have been obtained from

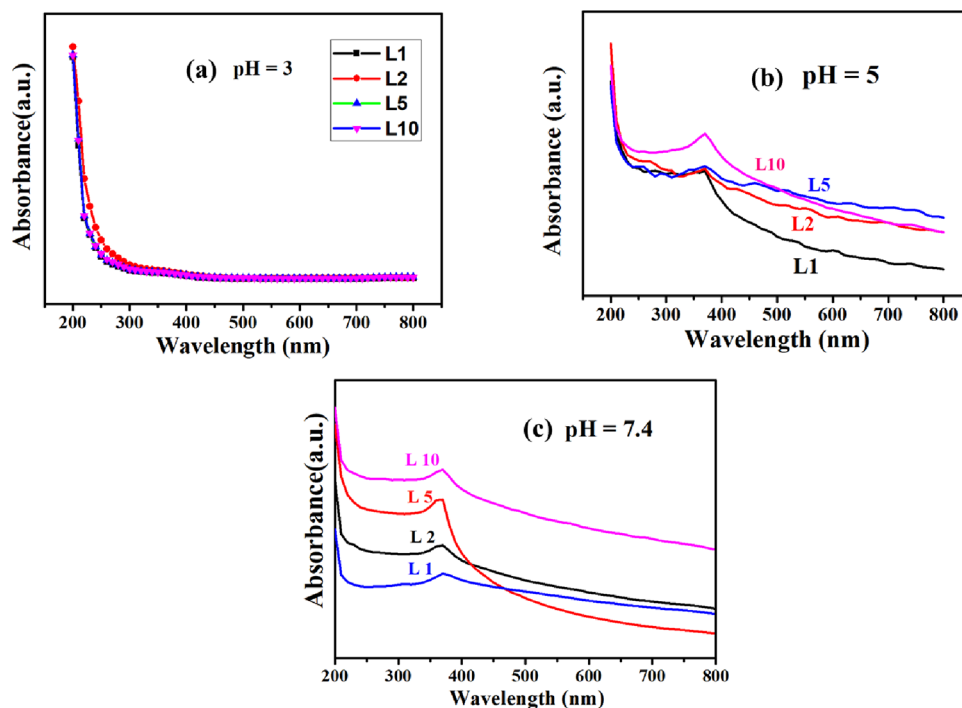


Figure 10. UV-visible absorbance spectra recorded at various pH values—(a) pH = 3, (b) pH = 5, and (c) pH = 7.4—for the synthesized ZnO (L1, L2, L5, and L10) nanoparticles.

Table 3. λ_{\max} Values of Various Green Synthesized ZnO Nanoparticles (L1, L2, L5, and L10) at Different pH Values

s. no.	ZnO nanoparticles	λ_{\max} (nm) (pH = 3)	λ_{\max} (nm) (pH = 5)	λ_{\max} (nm) (pH = 7.4)
1	L1		370	370
2	L2		370	370
3	L5		369	369
4	L10		368	368

Table 4. Band Gap Energy (E_g in eV) Obtained from Tauc Plots of Synthesized ZnO NPs with the Green Method

s. no.	ZnO nanoparticles	band gap energy E_g (eV)
1	L1	2.86
2	L2	2.80
3	L5	2.34
4	L10	2.28

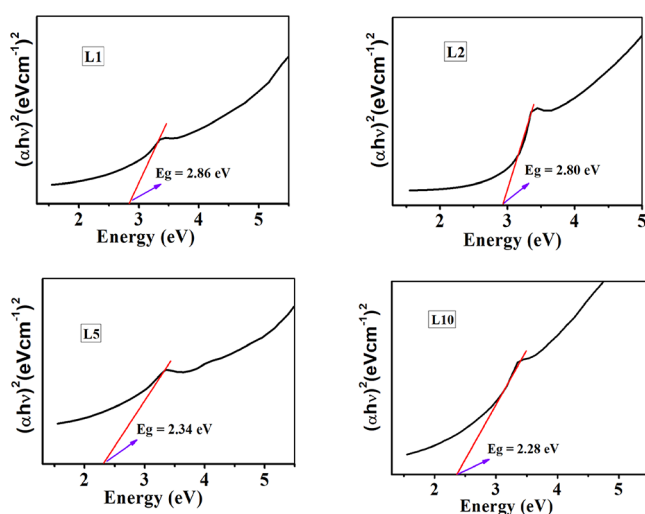


Figure 11. Tauc plots of synthesized ZnO NPs with the green method.

the MTT assay. The results of the MTT assay have determined the IC_{50} values as 141 $\mu\text{g/mL}$ for L1, 132 $\mu\text{g/mL}$ for L2, 127 $\mu\text{g/mL}$ for L5, and 115 $\mu\text{g/mL}$ for L10 nanoparticles. The anticancer activity of the leaf extract of *Azadirachta indica* increases as the amount of extract increases (as evidenced by

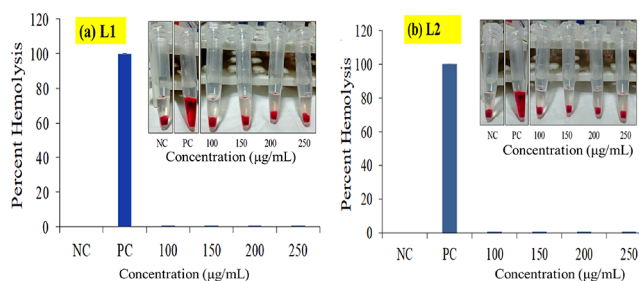


Figure 12. (a, b) Hemolytic effect of ZnO nanoparticles (L1 and L2) on erythrocytes. The representative photographs (inset) show the presence of hemoglobin in the supernatant of erythrocytes treated with L1 and L2, respectively, at different concentrations (100–250 $\mu\text{g/mL}$) for 1 h. Bar graphs in panels a and b represent the corresponding percent hemolysis with different concentrations of L1 and L2, respectively. NC: negative control (erythrocytes incubated with PBS) and PC: positive control (erythrocytes incubated with 0.2% Triton X-100). Data are shown as mean \pm SD.

the lower value of IC_{50} of L10 nanoparticles in this instance). In addition, the anticancer effect of L10 (at 250 $\mu\text{g/mL}$) has been observed to be more than that of the standard drug cisplatin (at 10 $\mu\text{g/mL}$). The biocompatibility of biosynthesized ZnO nanoparticles has been assessed using a hemolytic assay. Thus, biosynthesized ZnO (L1, L2, L5, and L10) nanoparticles have excellent potential to be used as promising

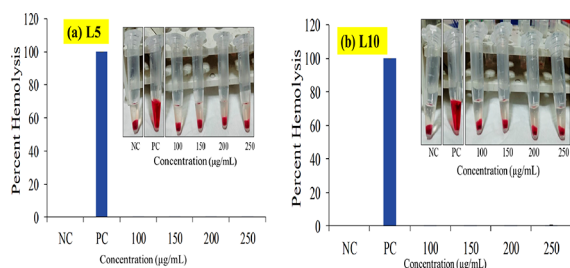


Figure 13. (a, b) Hemolytic effect of ZnO nanoparticles (L5 and L10) on erythrocytes. The representative photographs (inset) show the presence of hemoglobin in the supernatant of erythrocytes treated with L5 and L10, respectively, at different concentrations (100–250 $\mu\text{g/mL}$) for 1 h. Bar graphs in panels a and b represent the corresponding percent hemolysis with different concentrations of L5 and L10, respectively. NC: negative control (erythrocytes incubated with PBS) and PC: positive control (erythrocytes incubated with 0.2% Triton X-100). Data are shown as mean \pm SD.

clinical therapeutic agents for cervical cancer. In conclusion, for the clinical use of green synthesized ZnO nanoparticles for cancer treatment, an extensive *in vivo* study is needed for enhancing economic efficiency.

■ ASSOCIATED CONTENT

SI Supporting Information

The Supporting Information is available free of charge at <https://pubs.acs.org/doi/10.1021/acsomega.2c08302>.

The zeta potential plot of the biosynthesized ZnO (L1) nanoparticles (PDF)

■ AUTHOR INFORMATION

Corresponding Authors

Kalawati Saini – Department of Chemistry, Miranda House, University of Delhi, New Delhi 110007, India; orcid.org/0000-0002-0317-1935; Email: kalawati.saini@mirandahouse.ac.in

Anju Shrivastava – Department of Zoology, University of Delhi, New Delhi 110007, India; Email: anjushrivastavadu@gmail.com

Authors

Nutan Rani – Department of Chemistry, Miranda House, University of Delhi, New Delhi 110007, India

Kavita Rawat – Department of Zoology, University of Delhi, New Delhi 110007, India

Mona Saini – Department of Chemistry, Miranda House, University of Delhi, New Delhi 110007, India

Sapna Yadav – Department of Chemistry, Miranda House, University of Delhi, New Delhi 110007, India

Saima Syeda – Department of Zoology, University of Delhi, New Delhi 110007, India

Complete contact information is available at: <https://pubs.acs.org/doi/10.1021/acsomega.2c08302>

Author Contributions

Nutan Rani: conceptualization, methodology, original draft preparation; Kavita Rawat: experimental work for anticancer activity; Sapna Yadav: data interpretation and investigation; Mona Saini: UV-visible data and reference editing; Saima Syeda: hemolytic activity for biocompatibility; Anju Shriv-

astava: supervision of anticancer activity and hemolytic activity; Kalawati Saini: supervision, reviewing, and editing.

Funding

Sapna Yadav is thankful to CSIR, New Delhi, for providing a Senior Research Fellowship (Ref. 08/700(0004)/2019-EMR-1). Mona Saini would like to thank DBT, New Delhi, India, for providing a Junior Research Fellowship (Ref. BT/IN/Indo/Foldscope/39/2015 dated Mar 20, 2018).

Notes

The authors declare no competing financial interest.

■ ACKNOWLEDGMENTS

The authors express their sincere gratitude to the Principal, Miranda House, University of Delhi, for providing the lab to perform this research study.

■ LIST OF ABBREVIATIONS

AO, acridine orange; CV, crystal violet; DMEM, Dulbecco's modified Eagle medium; DMSO, dimethyl sulfoxide; DOX, doxorubicin; FBS, fetal bovine serum; HPV, human papillomaviruses; IC₅₀, concentration of nanoparticles at which 50% inhibition of cells occurs; MTT, 3-(4,5-dimethylthiazol-2-yl)-2,5-diphenyltetrazolium bromide; OD, optical density; PBS, phosphate buffer saline; PI, propidium iodide; ROS, reactive oxygen species; SiHa, cervical squamous carcinoma cell lines; TNBC, triple-negative breast cancer cells; ZnO, zinc oxide; VC, viable cells; SN, secondary necrosis; EA, early apoptosis; DLVO, Derjaguin–Landau–Verwey–Overbeek theory; RAW 264.7, murine macrophage cell lines (normal cell lines); NPs, nanoparticles

■ REFERENCES

- (1) Filippova, M.; Filippov, V.; Williams, V. M.; Zhang, K.; Kokoza, A.; Bashkurova, S.; Duerksen-Hughes, P. Cellular levels of oxidative stress affect the response of cervical cancer cells to chemotherapeutic agents. *BioMed Res. Int.* **2014**, *2014*, No. 574659.
- (2) Gowdhami, B.; Jaabir, M.; Archunan, G.; Suganthi, N. Anticancer potential of zinc oxide nanoparticles against cervical carcinoma cells synthesized via biogenic route using aqueous extract of *Gracilaria edulis*. *Mater. Sci. Eng., C* **2019**, *103*, No. 109840.
- (3) Wang, R.; Billone, P. S.; Mullett, W. M. Nanomedicine in action: an overview of cancer nanomedicine on the market and in clinical trials. *J. Nanomater.* **2013**, *2013*, No. 629681.
- (4) Misra, R.; Acharya, S.; Sahoo, S. K. Cancer nanotechnology: application of nanotechnology in cancer therapy. *Drug Discovery Today* **2010**, *15*, 842–850.
- (5) Prabhu, P.; Rao, M.; Murugesan, G.; Narasimhan, M. K.; Varadavenkatesan, T.; Vinayagam, R.; Chi, N. T. L.; Pugazhendhi, A.; Selvaraj, R. Synthesis, characterization and anticancer activity of the green-synthesized hematite nanoparticles. *Environ. Res.* **2022**, *214*, No. 113864.
- (6) Zhang, H.; Li, T.; Luo, W.; Peng, G. X.; Xiong, J. Green synthesis of Ag nanoparticles from *Leuciscus aspera* and its application in anticancer activity against alveolar cancer. *J. Exp. Nanosci.* **2022**, *17*, 47–60.
- (7) Hasanin, M.; Al Abboud, M. A.; Alawlaqi, M. M.; Abdelghany, T. M.; Hashem, A. H. Ecofriendly synthesis of biosynthesized copper nanoparticles with starch-based nanocomposite: antimicrobial, antioxidant, and anticancer activities. *Biol. Trace Elem. Res.* **2022**, *200*, 2099–2112.
- (8) Yang, Z.; Liu, Z.; Zhu, J.; Xu, J.; Pu, Y.; Bao, Y. Green synthesis and characterization of gold nanoparticles from *Pholiota adiposa* and their anticancer effects on hepatic carcinoma. *Drug Delivery* **2022**, *29*, 997–1006.

- (9) Bhatt, C. S.; Nagaraj, B.; Suresh, A. K. Nanoparticles-shape influenced high-efficient degradation of dyes: Comparative evaluation of nano-cubes vs nano-rods vs nano-spheres. *J. Mol. Liq.* **2017**, *242*, 958–965.
- (10) Iqbal, T.; Raza, A.; Zafar, M.; Afsheen, S.; Kebaili, I.; Alrobei, H. Plant-mediated green synthesis of zinc oxide nanoparticles for novel application to enhance the shelf life of tomatoes. *Appl. Nanosci.* **2022**, *12*, 179–191.
- (11) Subramanian, H.; Krishnan, M.; Mahalingam, A. Photocatalytic dye degradation and photoexcited anti-microbial activities of green zinc oxide nanoparticles synthesized via *Sargassum muticum* extracts. *RSC Adv.* **2021**, *12*, 985–997.
- (12) Kumar, A. Sol gel synthesis of zinc oxide nanoparticles and their application as nano-composite electrode material for super-capacitor. *J. Mol. Struct.* **2020**, *1220*, No. 128654.
- (13) Jayakumar, A.; Heera, K. V.; Sumi, T. S.; Joseph, M.; Mathew, S.; Praveen, G.; Nair, I. C.; Radhakrishnan, E. K. Starch-PVA composite films with zinc-oxide nanoparticles and phytochemicals as intelligent pH sensing wraps for food packaging application. *Int. J. Biol. Macromol.* **2019**, *136*, 395–403.
- (14) Dhawan, D. K.; Chadha, V. D. Zinc: a promising agent in dietary chemoprevention of cancer. *Indian J. Med. Res.* **2010**, *132*, 676–682.
- (15) Donga, S.; Chanda, S. *Caesalpinia crista* Seeds Mediated Green Synthesis of Zinc Oxide Nanoparticles for Antibacterial, Antioxidant, and Anticancer Activities. *BioNanoScience* **2022**, *12*, 451–462.
- (16) Suresh, J.; Pradheesh, G.; Alexramani, V.; Sundrarajan, M.; Hong, S. I. Green synthesis and characterization of zinc oxide nanoparticle using insulin plant (*Costus pictus D. Don*) and investigation of its antimicrobial as well as anticancer activities. *Adv. Nat. Sci.: Nanosci. Nanotechnol.* **2018**, *9*, No. 015008.
- (17) Rasmussen, J. W.; Martinez, E.; Louka, P.; Wingett, D. G. Zinc oxide nanoparticles for selective destruction of tumor cells and potential for drug delivery applications. *Expert opin. drug delivery* **2010**, *7*, 1063–1077.
- (18) Hanley, C.; Layne, J.; Punnoose, A.; Reddy, K. M.; Coombs, I.; Coombs, A.; Feris, K.; Wingett, D. Preferential killing of cancer cells and activated human T cells using ZnO nanoparticles. *Nanotechnology* **2008**, *19*, No. 295103.
- (19) Zhao, W.; Wei, J. S.; Zhang, P.; Chen, J.; Kong, J. L.; Sun, L. H.; Xiong, H. M.; Möhwal, H. Self-assembled ZnO nanoparticle capsules for carrying and delivering isotretinoin to cancer cells. *ACS Appl. Mater. Interfaces* **2017**, *9*, 18474–18481.
- (20) Govarthanan, M.; Srinivasan, P.; Selvankumar, T.; Janaki, V.; Al-Misned, F. A.; El-Serehy, H. A.; Kim, W.; Kamala-Kannan, S. Utilization of funnel-shaped ivory flowers of *Candelabra cactus* for zinc oxide nanoparticles synthesis and their in-vitro anti-cancer and antibacterial activity. *Mater. Lett.* **2020**, *273*, No. 127951.
- (21) Naser, R.; Abu-Huwaj, R.; Al-khateeb, I.; Abbas, M. M.; Atoom, A. M. Green synthesis of zinc oxide nanoparticles using the root hair extract of *Phoenix dactylifera*: Antimicrobial and anticancer activity. *Appl. Nanosci.* **2021**, *11*, 1747–1757.
- (22) Wu, H.; Zhang, J. Chitosan-based zinc oxide nanoparticle for enhanced anticancer effect in cervical cancer: A physicochemical and biological perspective. *Saudi Pharm. J.* **2018**, *26*, 205–210.
- (23) Rani, N.; Rawat, K.; Saini, M.; Yadav, S.; Shrivastava, A.; Saini, K.; Maity, D. *Azadirachta indica* leaf extract mediated biosynthesized rod-shaped zinc oxide nanoparticles for in vitro lung cancer treatment. *Mater. Sci. Eng., B* **2022**, *284*, No. 115851.
- (24) Rani, N.; Rawat, K.; Shrivastava, A.; Yadav, S.; Gupta, K.; Saini, K. In Vitro study of green synthesized ZnO nanoparticles on human lung cancer cell lines. *Mater. Today: Proc.* **2022**, *49*, 1436–1442.
- (25) Rani, N.; Rawat, K.; Saini, M.; Shrivastava, A.; Kandasamy, G.; Saini, K.; Maity, D. Rod-shaped ZnO nanoparticles: synthesis, comparison and in vitro evaluation of their apoptotic activity in lung cancer cells. *Chem. Pap.* **2022**, *76*, 1225–1238.
- (26) Jayakar, V.; Lokapur, V.; Nityasree, B. R.; Chalannavar, R. K.; Lasrado, L. D.; Shantaram, M. Optimization and green synthesis of zinc oxide nanoparticle using *Garcinia cambogia* leaf and evaluation of their antioxidant and anticancer property in kidney cancer (A498) cell lines. *Biomedicine* **2021**, *41*, 206–222.
- (27) Shwetha, U. R.; Latha, M. S.; Rajith Kumar, C. R.; Kiran, M. S.; Betageri, V. S. Facile synthesis of zinc oxide nanoparticles using novel *Areca catechu* leaves extract and their in vitro antidiabetic and anticancer studies. *J. Inorg. Organomet. Polym. Mater.* **2020**, *30*, 4876–4883.
- (28) Ratney, Y. J. J.; David, S. B. Evaluation of In-Vitro anticancer and antioxidant activity of Zinc Oxide nanoparticle by chemical and green method. *Int. J. Latest Trends Eng. Technol.* **2017**, 010–015.
- (29) Ostrovsky, S.; Kazimirsky, G.; Gedanken, A.; Brodie, C. Selective cytotoxic effect of ZnO nanoparticles on glioma cells. *Nano Res.* **2009**, *2*, 882–890.
- (30) Akhtar, M. J.; Ahamed, M.; Kumar, S.; Khan, M. M.; Ahmad, J.; Alrokayan, S. A. Zinc oxide nanoparticles selectively induce apoptosis in human cancer cells through reactive oxygen species. *Int. J. Nanomed.* **2012**, *7*, 845–857.
- (31) Lokapur, V.; Jayakar, V.; Divakar, M. S.; Chalannavar, R. K.; Lasrado, L.; Shantaram, M. ZnO nanoparticles with spectroscopically controlled morphology, bioinspired from *Hologarnagrahamii* (Wight) Kurz and delving its antioxidant and anticancer potential on A498 cell line. *Mater. Today Commun.* **2022**, *31*, No. 103338.
- (32) Bisht, G.; Rayamajhi, S. ZnO nanoparticles: a promising anticancer agent. *NANO* **2016**, *3*, 3–9.
- (33) Hill, J. M.; Speer, R. J. Organo-platinum complexes as antitumor agents. *Anticancer Res.* **1982**, *2*, 173–186.
- (34) Abdelmigid, H. M.; Hussien, N. A.; Alyamani, A. A.; Morsi, M. M.; AlSufyani, N. M.; Kadi, H. A. Green synthesis of zinc oxide nanoparticles using pomegranate fruit peel and solid coffee grounds vs. chemical method of synthesis, with their biocompatibility and antibacterial properties investigation. *Molecules* **2022**, *27*, 1236.
- (35) Al-Ghamdi, S. A.; Alkathiri, T. A.; Alfarraj, A. E.; Alatawi, O. M.; Alkathiri, A. S.; Panneerselvam, C.; Vanaraj, S.; Darwish, A. A. A.; Hamdalla, T. A.; Pasha, A.; Khasim, S. Green synthesis and characterization of zinc oxide nanoparticles using *Camellia sinensis* tea leaf extract and their antioxidant, anti-bactericidal and anticancer efficacy. *Res. Chem. Intermed.* **2022**, *48*, 4769–4783.
- (36) Ramón, L. A.; de la Cruz Hernández, E. N.; González, R. L.; Landero, M. F. H.; Owen, P. Q.; Mendoza, C. G.; Mendoza, G. M.; Lemus, M. A. A. Antiproliferative effect of 1, 10-Phenanthroline coupled to sulfated ZnO nanoparticles in SiHa cervix cancer cell line. *J. Sol-Gel Sci. Technol.* **2022**, *104*, 147–159.
- (37) Sadasivam, N.; Periakaruppan, R.; Sivaraj, R. Lantana aculeata L.-mediated zinc oxide nanoparticle-induced DNA damage in *Sesamum indicum* and their cytotoxic activity against SiHa cell line. *Phytotoxic. Nanopart.*; Springer 2018, 347–366, DOI: 10.1007/978-3-319-76708-6_15.
- (38) Anbu, A. S.; Velmurugan, P.; Lee, J. H.; Oh, B. T.; Venkatachalam, P. Biomolecule-loaded chitosan nanoparticles induce apoptosis and molecular changes in cancer cell line (SiHa). *Int. J. Biol. Macromol.* **2016**, *88*, 18–26.
- (39) Tripathi, D.; Modi, A.; Narayan, G.; Rai, S. P. Green and cost effective synthesis of silver nanoparticles from endangered medicinal plant *Withaniacoagulans* and their potential biomedical properties. *Mater. Sci. Eng., C* **2019**, *100*, 152–164.
- (40) Zhang, Y.; Zhang, X.; Zhang, L.; Alarfaj, A. A.; Hirad, A. H.; Alsabri, A. E. Green formulation, chemical characterization, and antioxidant, cytotoxicity, and anti-human cervical cancer effects of vanadium nanoparticles: A pre-clinical study. *Arab. J. Chem.* **2021**, *14*, No. 103147.
- (41) Ma, J.; Zhao, M.; Zhang, C.; Wu, X.; Yang, G. Synthesis of L. *Acidissima* mediated tin oxide nanoparticles for cervical carcinoma treatment in nursing care. *J. Drug Delivery Sci. Technol.* **2020**, *57*, No. 101745.
- (42) Govindasamy, R.; Govindarasu, M.; Alharthi, S. S.; Mani, P.; Bernaurdshaw, N.; Gomathi, T.; Ansari, M. A.; Alomary, M. N.; Atwah, B.; Malik, M. S.; Rajeswari, V. D.; Rekha, K.; Ahmed, S. A.; Thiruvengadam, M. Sustainable green synthesis of yttrium oxide (Y₂O₃) nanoparticles using Lantana camara leaf extracts: Physico-

chemical characterization, photocatalytic degradation, antibacterial, and anticancer potency. *Nanomaterials* **2022**, *12*, 2393.

(43) Siddiquee, M. A.; ud din Parray, M.; Mehdi, S. H.; Alzahrani, K. A.; Alshehri, A. A.; Malik, M. A.; Patel, R. Green synthesis of silver nanoparticles from *Delonix regia* leaf extracts: In-vitro cytotoxicity and interaction studies with bovine serum albumin. *Mater. Chem. Phys.* **2020**, *242*, No. 122493.

(44) Arakha, M.; Roy, J.; Nayak, P. S.; Mallick, B.; Jha, S. Zinc oxide nanoparticle energy band gap reduction triggers the oxidative stress resulting into autophagy-mediated apoptotic cell death. *Free Radical Biol. Med.* **2017**, *110*, 42–53.